Pelosini, L., Hull, C., Boyce, J. F., McHugh, D., Stanford, M. R. & Marshall, J. (2011). Optical Coherence Tomography May Be Used to Predict Visual Acuity in Patients with Macular Edema. Investigative Ophthalmology & Visual Science, 52(5), pp. 2741-2748. doi: 10.1167/iovs.09-4493


CITY UNIVERSITY LONDON

City Research Online

# Optical Coherence Tomography maybe used to predict Visual Acuity in patients with Macular Oedema

Lucia Pelosini[1], Christopher C Hull[2], James F Boyce[1], Miles R Stanford[1], John Marshall[1]

[1]Department of Ophthalmology, Kings College London, Rayne Institute, St Thomas' Hospital, London, Lambeth Palace Road, London, SE1 7EH

[2]Department of Optometry & Visual Science, City University, London

Grant information: The present study was funded by a grant of The Royal College of Surgeons, London, United Kingdom

Disclosure:

JM is a paid consultant for OTI (Ophthalmic Technologies Inc., Toronto, Canada)

None of the other authors have a financial interest in the subject of the presentation.

Word count:

Key words: cystoid macular oedema; optical coherence tomography (OCT); spectral OCT; coronal (en-face) OCT; central macular thickness; ocular imaging.

**Abstract**

**Purpose:** To determine whether the volume of retinal tissue passing between the inner and outer retina in macular oedema could be used to predict visual acuity.

**Methods:** Diabetic and uveitic patients with cystoid macular oedema (81 subjects, 129 eyes) were recruited. Best corrected LogMAR visual acuity and spectral optical coherence tomography (OCT/SLO OTI, Toronto) were performed for all patients. Coronal OCT scans obtained from a cross-section of the retina between the plexiform layers were analyzed using a grid of 5 concentric radii (500µ, 1000µ, 1500µ, 2000µ, 2500µ centred on the fovea). The images were analyzed to determine the amount of retinal tissue present within each ring. A linear regression model was developed to determine the relationship between tissue integrity and LogMAR visual acuity.

**Results:** The volume of retinal tissue between the plexiform layers in ring 1 and 2 (up to 1000 µ from the foveal centre) predicted 80% of the change in visual acuity using a linear model. By contrast, central macular thickness within the central 1000 µ predicted only 14% of the change in visual acuity.

**Conclusions:** This study showed that the cross-sectional area of retinal tissue between the plexiform layers in cystoid macular oedema, as imaged by OCT, is a much better predictor of visual acuity at baseline than central macular thickness. Further prospective treatment trials are required to investigate this parameter as a predictor of visual outcome after intervention.

## Introduction

Macular oedema results from abnormal accumulation of fluid in the central retina and indicates compromised function in one or both of the blood retinal barriers. It is a common sequel of many ocular conditions and the main cause of visual loss in diabetic retinopathy[1-5].

Any abnormal pooling of extracellular fluid may result in displacement of the spatial relationships between retinal neuronal components. Small amounts of fluid may lead to an increase in overall retinal thickness, whilst larger amounts may give rise to cell free spaces as seen in cystoid macular oedema[5].

Observations from histology and optical coherence tomography (OCT) give a false impression of multiple cysts delineated by tissue structures in the Z-plane of the retina (Figure 1). However, scanning electron microscopy shows that more commonly a single cystic space is present within which a number of structures extend from the inner to the outer retina (Figure 2). Such structures consist of columns of Muller's fibres together with the axonal elements of bipolar cells passing between the two plexiform layers[6]. Empirical studies have demonstrated that the two plexiform layers together with the outer limiting membrane form a physical resistance barrier to fluid movements[7]. Thus, extracellular fluid may be contained within layers defined by these resistance barriers. In diabetic retinopathy, cystic spaces may occur either between the inner and the outer plexiform layers or between the outer limiting membrane and the outer plexiform layer. In the former location, there is a potential to displace bipolar cells leading to cell loss or compromised function, whilst in the latter, only photoreceptor cells are at risk[8, 9].

Given the fundamental role of bipolar cells in being the sole communication pathway between photoreceptors and ganglion cells, any loss of connectivity between these

cells will compromise visual function[10, 11]. It follows that the more the retinal thickness increases, the more such axons will be stretched and as a consequence some will break. This is probably the mechanism underlying the apparent relationship between increasing retinal thickness and decreasing visual acuity. By contrast, those bipolar cells whose axons are closely adjacent to Muller's fibres will have a greater chance of surviving displacement because of the greater physical strength and support provided by the adjacent Muller's fibres[11-16].

Theoretically, a useful indicator of the visual acuity and potential visual outcome in eyes with macular oedema would be to analyze the residual volume of tissue passing between the two plexiform layers, as only such areas would allow passage of bipolar axons between photoreceptors and ganglion cells. The impact of photoreceptor-ganglion cell connectivity on visual acuity would further depend upon the location of surviving axons within the central visual field[17]. Thus an optimal measurement of potential function would be an evaluation of the number of vertical elements passing between the plexiform layers, their diameter and eccentricity from the fovea.

This study had two objectives: 1) to assess new hardware for imaging retinal glial tissue in cases of cystoid macular oedema 2) to investigate whether the amount of glia and by association residual bipolar cells could be used as indicator of visual function in patients with cystoid macular oedema.

## Methods

### Experimental design

Patients with macular oedema were prospectively recruited from both diabetic and uveitic outpatient clinics over a period of nine months. The study involved a baseline assessment of visual function, ophthalmoscopy and OCT imaging at a single timepoint. The research conformed to the tenets of the Declaration of Helsinki with informed consent being obtained from the subjects subsequent to explanation of the nature of the study. The protocol of the study was approved by the local ethics committee (Protocol number: 06/Q0702/175).

Patient information was anonymized at the time of patient recruitment to allow indipendent data analysis.

Inclusion criteria for the study were a clinical diagnosis of cystoid macular oedema (CMO), confirmed either by OCT alone or by OCT and fundus fluorescein angiography (FFA) at the time of enrolment. For each patient either one or both eyes were included in the study.

Patients with coexisting ocular pathologies were excluded. Exclusion criteria included the presence of media opacity affecting the quality of the OCT scan and angiographic or clinical evidence of ischaemic maculopathy.

### Subjects and clinical procedures

Each patient underwent a complete anterior segment examination by slit-lamp biomicroscopy and best corrected visual acuity assessment using a LogMAR chart at 3 metres distance. All patients were then dilated using Phenylephrine 2.5% and Tropicamide 1% and examined by indirect fundoscopy with a 78D lens. In the diabetic patients, fluorescein angiography was required as one of the inclusion criteria

of the study in order to assess retinal circulation and to allow exclusion of patients with subclinical foveal ischaemia.

**Optical Coherence Tomography**

Optical coherence tomography was carried out using a Spectrum-OTI spectral domain OCT/SLO system (Spectral OCTSLO model E, Spectrum-Ophthalmic Technologies Inc., Toronto, Canada). This device is an optical imaging system, combining a Confocal Scanning Ophthalmoscope and Optical Coherence Tomography. Both the confocal fundus SLO image and the OCT image are generated through the same optics and displayed simultaneously on the computer screen with pixel to pixel correspondence. The system uses light generated from an infrared broadband super luminescent diode (SLD) with a wavelength between 790nm and 950nm. Cross-sectional images of the retina along the x-y plane (B-Scan), such as single line, radial and raster scans, could be obtained as well as coronal images within the z plane (C-scan).

In preliminary studies, scans were obtained using three different modes of operation. First, a series of 24 radial scans over 360 degrees were automatically initiated intersecting at the centre of the patient's fixation. Secondly, a single scan mode was selected whose orientation and location within the fundus was determined by the operator. Thirdly, the system was used to generate a raster scan of the macula from the superior to the inferior arcade with 64 scans, again centred by the patient's fixation.

Three dimensional views of the macula were obtained by selecting the topography mode where images were viewed as surface maps and these were extracted manually by slicing the 3-D picture using the device based image analysis software. The topography scan also allowed the operator to extract information about retinal

thickness in different areas of the posterior pole by using the ETDRS macular grid. Coronal scans (C-scans) were fundamental to the present study and obtained by selecting the mid point between the ganglion cell layer and the innermost aspect of the outer plexiform layer, in most cases to mid depth of the cysts. In practice this was obtained by adjusting the section plane to an appropriate level parallel with the retinal surface in the B scan displayed on the x-axis of the coronal image (Figure 3A).

**Image analysis**

To investigate the purpose of this study, three pieces of information were required from each patient: 1) the number of columns of tissue present 2) their cross-sectional area at their narrowest point 3) their eccentricity from the foveal centre.

An image analysis system was created to extract each of these datasets. Data were collected from a series of concentric rings of 500 µm, 1000 µm, 1500 µm, 2000 µm, 2500 µm radii respectively (Figure 3B). Thus, within each ring, the area of surviving tissue as opposed to cystic space was extracted by first compressing the greyscale such that tissue became white and oedema black[18]. The second part of the program counted the number of white pixels present within each ring thus giving a measure proportionate to the potential number of connections passing between the two plexiform layers. The number of pixels of spared tissue within each annulus was converted to an area in $mm^2$ by scaling the ratio of the number of pixels of spared tissue to the total number of pixels in the annulus by the area in $mm^2$ of the annulus.

**Outcome measures**

This study had three primary outcomes: 1) Best corrected Log MAR visual acuity; 2) retinal tissue integrity evaluated as number of pixels corresponding to the tissue component between cystic spaces and observable at increasing eccentricities from the

fovea in segmented images of OCT/SLO coronal scans; and 3) central macular thickness measurement obtained from the OCT/SLO retinal thickness map.

**Statistics**

All data organization and manipulation was carried out in Microsoft® Office Excel 2003 (Microsoft, Redmond, WA) and statistical analysis was performed using SPSS 16.0 for Windows (SPSS Inc, Chicago, IL) and MINITAB Release 13.30 (MINITAB Inc, State College, PA). Following tests for normality, (Kolmogorov-Smirnov test; $P < 0.05$ considered statistically significantly different from normal), correlation coefficients were calculated to evaluate the association between visual acuity and the other 6 outcome measures.

A linear regression model was developed to assess if the amount of glia could be used to predict visual acuity. The data set of 129 eyes were randomised and split into two data sets, one of 100 eyes and the other of 29 eyes. A stepwise linear regression was performed on the data set of 100 eyes with logMAR visual acuity as the dependent variable and the other 6 outcome measures as predictors. The criterion for entry into the model was $P = 0.05$ and $P = 0.10$ for removal. Stepwise linear regression is an extension of simple linear regression where the dependent variable is predicted by a linear equation involving one outcome or independent variable and a constant. In stepwise linear regression, multiple variables can be linearly combined in the model. They are entered automatically by the statistics software provided they make a statistically significant improvement in the model. Stepwise linear regression has been used in a large number of areas[19].

The remaining 29 eyes were used to test the model by assessing the agreement between the predicted and measured visual acuity using the Bland-Altman method[20].

## Results

A total of 81 participants enrolled, 36 males and 45 females. The average age was 63 years (range 26-87 years) (Table 1).

Most patients (73%, 59 subjects) underwent fluorescein angiography, whereas in the remaining group an angiographic study could not be performed (27%, 22 subjects) due to previously documented adverse reaction to the dye (9 subjects), refusal to the investigation (8 subjects) or technical difficulty to obtain a satisfactory venous access (7 subjects). Typical patient contact time was 40 minutes of which only 5 minutes were required for OCT imaging.

### Relationship between tissue integrity and visual function

The scatter plots in figure 4 (b & c) show a linear relationship between the amount of spared tissue within rings 1 and 2 and Log MAR visual acuity. The correlation falls progressively for rings 3, 4 and 5 (Figure 4 d,e & f). Not all variables were normally distributed (P = 0.000 to 0.200) therefore Spearman rank correlation coefficients were calculated[21] Their values, together with the associated statistical significance and the $R^2$ values are given in table 2. $R^2$ values are reported since they give the percentage of the variation in visual acuity explained by the outcome measures (central macular thickness or the tissue sparing within each of the 5 rings).

**Relationship between macular thickness and visual function**

The relationship between central macular thickness (CMT) and visual acuity is shown in the scatter plot in Figure 4(a). The correlation between CMT and LogMAR visual acuity was moderate ($r_s$ = 0.407). The coefficient of determination ($R^2$ value) demonstrates that CMT only explains 16.6% of the change in visual acuity using a linear model (Table 2).

**Linear Regression Model**

The linear regression model following stepwise linear regression was given by

$$\log \mathrm{MAR} = 1.091 + 0.271 \times \mathrm{CMT} - 0.548 \times \mathrm{T1} - 0.289 \times \mathrm{T2} \qquad (1)$$

where CMT was the central macular thickness in mm and T1 and T2 were the areas of tissue sparing in $mm^2$ in rings 1 and 2 respectively. This model had an $R^2$ value of 80.7% indicating that equation (1) accounted for over 80% of the variation in LogMAR visual acuity. It was noteworthy that the most predictive variable was T2 and this alone could predict 74.4% of the variation in LogMAR visual acuity using a linear model. The significance of this result will be commented on further in the discussion.

Figure 6 shows the results of testing the model and is a scatter plot of the measured Log MAR visual acuity plotted against the estimated LogMAR visual acuity using equation (1). A line of equality is shown along which all data points would be expected to lie in presence of perfect agreement. Clearly this was not the case, as expected from most clinical measures.

Figure 7 shows the Bland-Altman mean-difference plot for our data. It demonstrates a bias of -0.02 logMAR units and limits of agreement of ±0.23 logMAR units.

## Discussion

This study has demonstrated that there is a strong correlation between visual acuity in patients with cystoid macular oedema and the volume of tissue passing between the two plexiform layers in the central retina as determined by OCT. It is the first time that a predictive measure of visual performance has been derived from imaging of macular oedema.

The results demonstrate that good visual acuity only occurred in those patients with an adequate volume of tissue running between the inner and the outer plexiform layers in the central 1000-2000µ of retina (Figure 4 and 5). Given that foveal cones have inner connecting fibres that may be up to 500µm in length[17] foveolal cones may connect to bipolar cells displaced 500µm radially from the inner and outer segments. Thus this lateral displacement of connections between foveal cones and ganglion cells explains the dependency of visual acuity on the tissue integrity in both rings 1 and 2.

While there was still reasonable correlation within ring 3, presumably due to signals derived from photoreceptors at the extreme edges of the fovea, correlation was lost within rings 4 and 5. In these locations, although large amounts of tissue volume may be spared, the connectivity is predominantly with extrafoveal photoreceptors.

These findings are in keeping with both an anatomical study looking at displacement of retinal ganglion cells subserving cones in the human fovea[17] and a pathological study measuring laser damage to foveal photoreceptor cells[21]. Sjostrand et al measured the radial offset produced by cone fibres within the layer of Henle and demonstrated that at the foveal border (0.5-0.8 mm or 1.8-2.9 deg eccentricity) the mean offset due to fibres of Henle and mean total lateral displacement was at a maximum of 0.32±0.03 mm and 0.37±0.03 mm respectively, thereafter steeply decreasing outside the foveal border out to an eccentricity of 2-2.5 mm. This

anatomical finding confirms that structural damage involving the neural retina up to 1mm from the foveal centre might have implications for loss of information generated within the fovea.

In order to estimate the number of axonal elements necessary to maintain potential for visual function, more information is needed with regard to the spatial arrangement of bipolar and Muller fibres in the residual columns and their relative ratio. From electron microscopy studies it is known that bipolar axons are surrounded by Muller fibres in the human retina[22]. Given that the approximate diameter of bipolar axons is 0.5μ and the diameter of Muller fibres is between 5μ and 10μ, we can estimate that in normal conditions for each Muller fibre there are approximately 34 to 68 adjacent bipolar neurones around their circumference.

By contrast, in pathological conditions such as macular oedema, accumulation of intracellular fluid may reduce the total number of Muller fibres but may also result in an increase in the diameter of those remaining up to 15-20μ. This would allow an increase in the potential number of surrounding bipolar axons to approximately 97 to 128 (Figure 2).

Furthermore, from the linear regression model, it appears that a minimum of 50% of preserved retinal tissue within ring 1 is necessary in order to maintain a visual acuity of 0.4 LogMAR or better (Figure 4, scatter plot b), whereas at least 70% of the retinal tissue within ring 2 is necessary for a level of visual acuity of 0.4 LogMAR or better (Figure 4, scatter plot c).

Even though the total number of bipolar axons traversing the space between the plexiform layers may be significantly reduced, both horizontal and amacrine cells will contribute to image processing and VA by integrating signals over a number of photoreceptor cells and ganglion cells respectively.

The major source of error in the present study is the potential loss of information implicit in compression of greyscale during the image analysis. At extremes, potential connectivity may be lost if too few pixels are present in a given element within the primary image to be resolved as tissue. By contrast, some discontinuous elements which do not really traverse the interplexiform space may be interpreted as intact elements. Further work is therefore required to optimize the image analysis process and to give further maximal and minimal correlates for axonal elements potentially associated with the glial tissue.

In the present paper, no attempt has been made to determine degradation of visual information resulting from fluid accumulation either beneath the retinal pigment epithelium or beneath the interphotoreceptor matrix. Clearly, the potential visual acuity of any given patient relates to both the quality of the image presented to the photoreceptor cells and the ability to transmit such resolved information from the photoreceptors to the ganglion cells.

The former may well be degraded by the presence of fluid in the outer retina, whilst the latter will be less dependent upon fluid distribution in the inner retina and more dependent on the number of viable bipolar axons.

Recovery or improvement of visual acuity may be dependent on changes induced in both these components. First, some improvement may occur resulting from removal of fluid from the outer retinal layers as a consequence of changing fluid and ionic environment in the inter-photoreceptor matrix thus potentially enhancing transduction. Secondly, whilst no current therapeutic regime will replace lost neurones, drainage of the cystoid fluid will remove tension on the axons passing through the cysts and at the same time change the ionic environment around the axons and both of these may enhance function. Given the role of the Muller fibres in

transretinal transport of ions[23], changes to their environment maybe of particular importance.

Several studies have investigated the value of various objective parameters derived from images of macular oedema as indicators of visual function[24-29]. Using fluorescein angiograms, Arend at al investigated the relationship between the mean area of the cysts and number of cystic spaces in cystoid macular oedema with measures of visual acuity, demonstrating a significant correlation ($R^2$ 0.61 and 0.48 respectively) [29]. Other authors investigated patterns of fluid distribution in macular oedema as a predictor of visual funtion with little success [30].

At present, the measurement of retinal thickness with OCT represents the accepted standard despite its incredibily poor correlation with visual function ($R^2$ values ranging from 0.08 to 0.54) compared with the results presented in the current paper[31]. The relationship between macular thickness and visual acuity has also shown poor consistency across different studies[31-37].

The apparent correlation between the increase in retinal thickness and the decrease in visual acuity may be explained by the results of the present paper whereby increase in thickness will be associated with increase in loss in viable axons. The more direct approach to assessing neuronal survival in the present study would also explain why the correlation values are so much better.

The present study validates retinal tissue integrity as a measure of preserved axonal connections and indicator of visual function. The strength of the relationship between preserved tissue and visual function, as expected, decreases at increasing eccentricities from the centre of the fovea.

It will be of interest to apply the current analysis to future trials of regimens designed to modulate oedema. The ability to determine the potential visual outcome for patients

prior to the commencement of any treatment trial will be highly beneficial in that it will allow exclusion of those individuals who could not in anyway benefit from intervention. A longitudinal treatment trial is necessary in order to validate the assessment of retinal structural integrity at baseline and to relate this parameter to the the final visual outcome.

**References**


1. Gass JD, Anderson DR, Davis EB. A clinical, fluorescein angiographic, and electron microscopic correlation of cystoid macular edema. Am J Ophthalmol. 1985;100:82–86.
2. Gass JDM, Norton EDW. Cystoid macular edema and papilledema following cataract extraction: a fluorescein fundoscopic and angiographic study. Arch Ophthalmol. 1966;221–224.
3. Yanoff M, Fine BS, Brucker AJ, Eagle RCJr. Pathology of human cystoid macular oedema. Surv Ophthalmol. 1984;28:505-511.
4. Fine BS, Brucker AJ. Macular edema and cystoid macular edema. Am J Ophthalmol. 1981;92:466-481.
5. Antcliff R, Marshall J. The pathogenesis of edema in diabetic maculopathy. Seminars in Ophthalmology. 1999;14:223-232.
6. Marshall J. The effects of ultraviolet radiation and blue light on the eye. Macmillan Press, Ltd. The Susceptible Visual Apparatus. London, 1991, 54-92
7. Antcliff RJ, Hussain AA, Marshall J: Hydraulic conductivity of fixed retinal tissue after sequential excimer laser ablation: barriers limiting fluid distribution and implications for cystoid macular edema. Arch Ophthalmol. 2001;119:539–544.
8. Hee MR, Puliafito CA, Duker JS et al. Topography of diabetic macular edema with optical coherence tomography. Ophthalmology. 1998;105:360–370.
9. Hee MR, Puliafito CA, Wong C et al. Quantitative assessment of macular oedema with optical coherence tomography. Arch Ophthalmol. 1995;113(8):1019-1029.

10. Yamada E. Some structural features of the fovea centralis in the human retina. Arch Ophthalmol. 1969;82:151-159.
11. Gass JDM. Muller cell cone, an overlooked part of the anatomy of the fovea centralis. Arch Ophthalmol. 1999;117:821-823.
12. Otani T, Kishi S, Maruyama Y. Patterns of diabetic macular edema with optical coherence tomography. Am J Ophthalmol. 1999;127(6):688-931.
13. Kim BY, Smith SD, Kaiser PK. Optical coherence tomographic patterns of diabetic macular oedema. Am J Ophthalmology. 2006;142(3):405-412.
14. Gibram SK, Khan K, Jungkim S, Cleary PE. Optical coherence tomographic pattern may predict visual outcome after intravitreal triamcinolone for diabetic macular edema. Ophthalmol. 2007;114:890-894.
15. Goebel W, Kretzchmar-Gross T. Retinal thickness in diabetic retinopathy: a study using optical coherence tomography (OCT). Retina. 2002;22:759–67.
16. Hee MR, Puliafito CA, Wong C, et al. Quantitative assessment of macular edema with optical coherence tomography. Arch Ophthalmol. 1995;113:1019–29.
17. Sjostrand J, Popovic Z, Conradi N, Marshall J. Morphometric study of the displacement of retinal ganglion cells subserving cones within the human fovea. *Graefe's Arch Clin Exp Ophthalmol*. 1999;237:1014-1023.
18. Barman SA, Hollick EJ, Boyce JF, Spaton DJ, Uyyanonvara B, Sanguinetti G, Meacock W. Quantification of posterior capsular opacification in digital images after cataract surgery. Invest Ophthalmol Vis Sci. 2000;41(12):3882-3892.
19. Altman DG, "Practical Statistics for Medical Research," Chapman & Hall, London, 1991.
20. Bland JM, Altman DG. Measuring agreement in method comparison studies. Stat Meth Med Res. 1999;8:135-160.

21. Marshall J, Hamilton AM, Bird AC. Histopathology of ruby and argon laser lesions in monkey and human retina. A comparative study. Br J Ophthalmol. 1975;59:610-630.

22. Hogan MJ, Alvarado JA, Weddell JE. Histology of the human eye: an atlas and textbook. WB Saunders, Philadelphia, 1971.

23. Biedermann B, Skatchkov SN, Brunk I, Bringmann A, Pannicke T, Bernstein HG, Faude F, Germer A, Veh R, Reichenbach A. Spermine/spermidine is expressed by retinal glial (Mueller's) cells and controls distinct K+ channels of their membrane. Glia.1998;23(3):209-220.

24. Smith RT, Lee CM, Charles HC, Farber M, Cunha-Vaz JG. Quantification of diabetic macular edema. Arch Ophthalmol. 1987;105:218-22.

25. Puliafito CA, Hee MR, Lin CP, Reichel E, Schuman JS, Duker JS, Izatt JA, Swanson EA, Fujimoto JG. Imaging of macular diseases with optical coherence tomography. Ophthalmology. 1995;102:217-29.

26. Ko TH, Fujimoto JG, Schuman JS et al. Comparison of ultrahigh- and standard-resolution optical coherence tomography for imaging macular pathology. Ophthalmology. 2005;112:191–197.

27. Catier A, Tadayoni R, Paques M et al. Characterization of macular edema from various etiologies by optical coherence tomography. Am J Ophthalmol. 2005;140:200–206.

28. Massin P, Duguid G, Erginay A et al. Optical coherence tomography for evaluating diabetic macular edema before and after vitrectomy. Am J Ophthalmol. 2003;135:169 –177.

29. Arend O, Remky A, Elsner AE, Betram B, Reim M, Wolf S. Quantification of cystoid changes in diabetic maculopathy. IOVS 1995;36:608-613.

30. Otani T, Kishi S. Correlation between optical coherence tomography and fluorescein angiography findings in diabetic macular oedema. Ophthalmology. 2007;114(1):104-107.
31. Diabetic Retinopathy Clinical Research Network. Relationship between optical coherence tomography-measured central retinal thickness and visual acuity in diabetic macular oedema. Ophthalmology. 2007;114:525-536.
32. Nussenblatt RB, Kaufman SC, Palestine AG et al: Macular thickening and visual acuity. Measurement in patients with cystoid macular edema. Ophthalmology. 1987;94:1134–1139.
33. Larsson J, Zhu M, Sutter F, Gillies MC. Relation between reduction of foveal thickness and visual acuity in diabetic macular edema treated with intravitreal triamcinolone. Am J Ophthalmol. 2005;139(5):802-806.
34. Massin P, Erginay A, Haouchine B et al. Retinal thickness in healthy and diabetic subjects measured using optical coherence tomography mapping software. Eur J Ophthalmol. 2002;12:102–108.
35. Yang CS, Cheng CY, Lee FL et al. Quantitative assessment of retinal thickness in diabetic patients with and without clinically significant macular edema using optical coherence tomography. Acta Ophthalmol Scand. 2001;79:266–270.
36. Schaudig UH, Glaefke C, Scholz F et al. Optical coherence tomography for retinal thickness measurement in diabetic patients without clinically significant macular edema. Ophthalmic Surg Lasers. 2000;31:182–186.
37. Browning DJ, Glassman AR, Aiello LP et al. Optical coherence tomography measurements and analysis methods in optical coherence tomography studies of diabetic macular oedema. Ophthalmology. 2008;115(8):1366-1371.

**Legends**

**Figure 1**: Light microscopy and optical coherence tomography (OCT/SLO, OTI, Toronto) images of human retina affected by cystoid macular oedema (CMO). Examples of early (top photo) and late CME (bottom photo) are represented. Intraretinal fluid appears contained in cystic spaces separated by walls.

**Figure 2**: Scanning electron microscopy of cystoid macular oedema. Columns of tissue are standing up in a continuous space of fluid pooling. Retinal elements along the z-plane are represented by bipolar axons and Muller fibres (Prof J Marshall's collection).

**Figure 3**: (3A) Macular thickness map of a patient with macular oedema representing subfield mean thicknesses as from ETDRS study; (3B) Grayscale coronal OCT scan with superimposed grid dividing the macula in 5 areas of increasing eccentricity (radii:500µ, 1000µ, 1500µ, 2000µ, 2500µ).

**Figure 4**: Scatter plots showing the relationship between a) Central macular thickness versus LogMAR VA ($r_s$ = 0.407*); b) Tissue integrity within circle 1 versus LogMAR VA ($r_s$ = -0.832*); c) Tissue integrity within circle 2 versus LogMAR VA ($r_s$ = -0.841*); d) Tissue integrity within circle 3 versus LogMAR VA ($r_s$ = -0.624*); e) Tissue integrity within circle 4 versus LogMAR VA ($r_s$ = -0.277*); f) Tissue integrity within circle 5 versus LogMAR VA ($r_s$ = -0.134). *correlation is significant at the 0.05 level (2-tailed)

**Figure 5**: Variation in $R^2$ values, representing the association between visual acuity and retinal spared tissue at increasing eccentricity as well as visual acuity and central macular thickness (CMT)

**Figure 6** Scatter plot, with line of equality, for measured versus predicted LogMAR visual acuity using the linear regression model developed in this study

**Figure 7** Bland-Altman mean-difference plot demonstrating agreement between measured and predicted LogMAR visual acuity

**Table 1**: Baseline clinical characteristics of study subjects

**Table 2:** Regression values and Spearman correlation coefficients describing the relationship between the outcome measures and LogMAR visual acuity for all 129 eyes in the study.

**Figure 1**

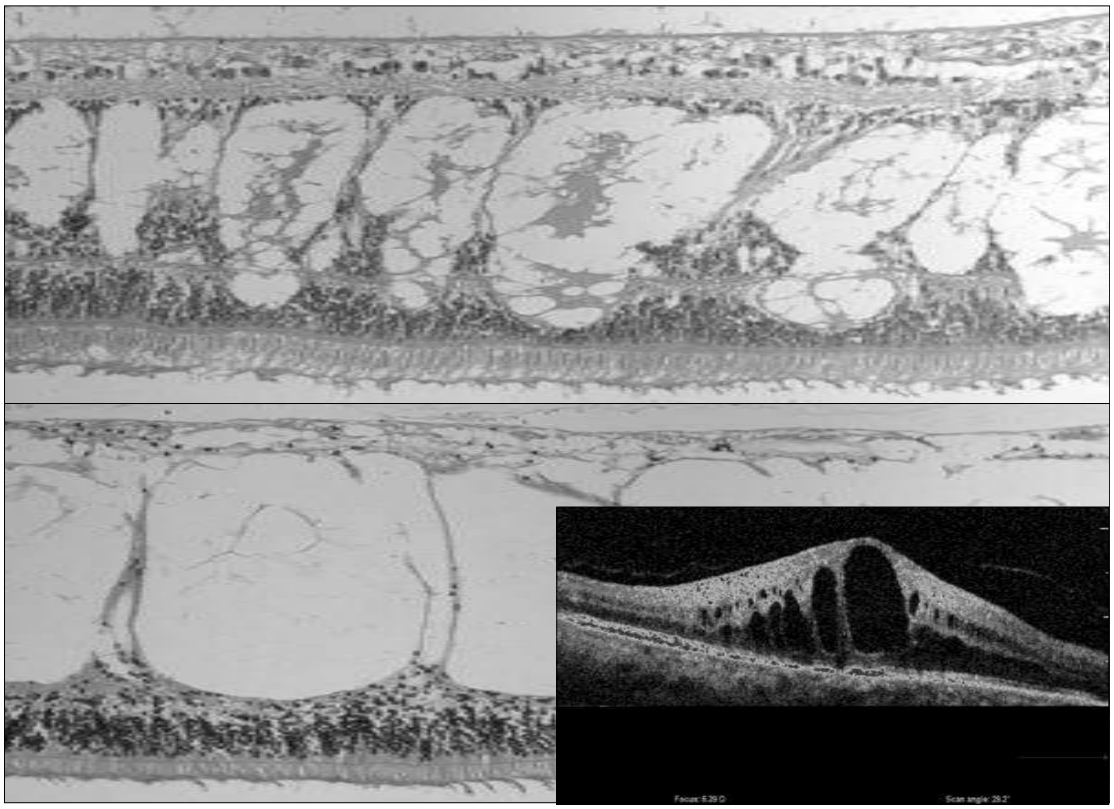

**Figure 2**

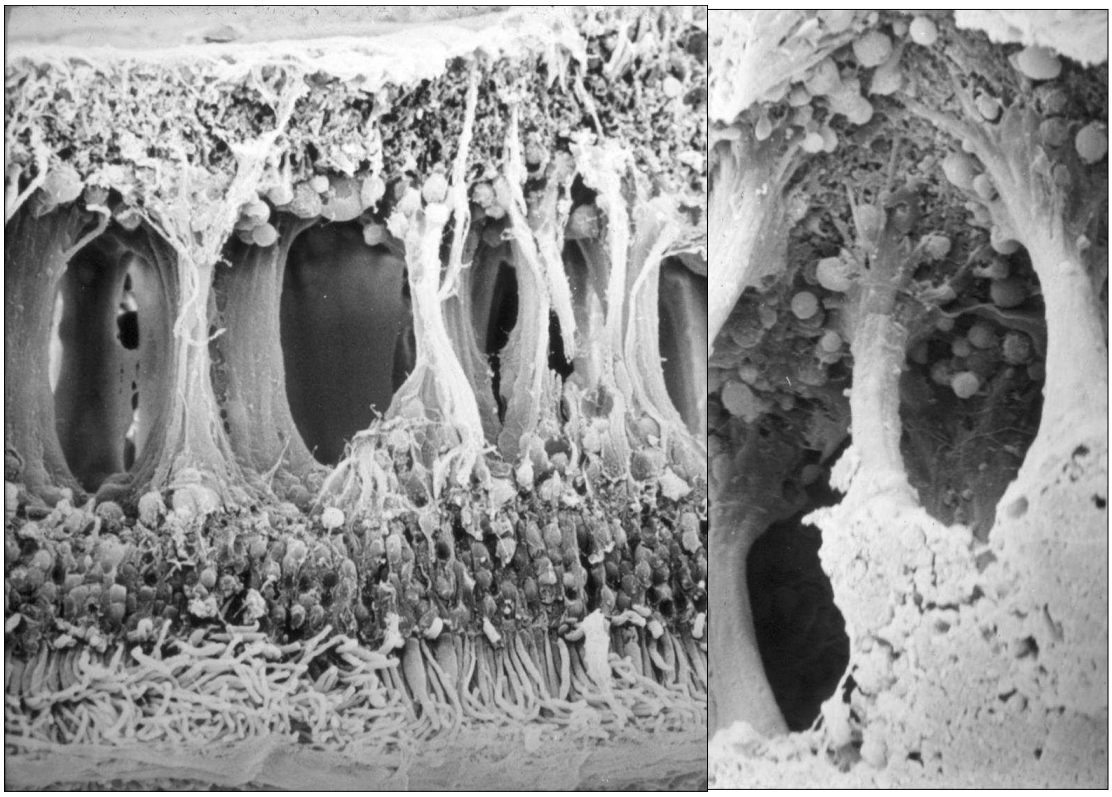

**Figure 3A**

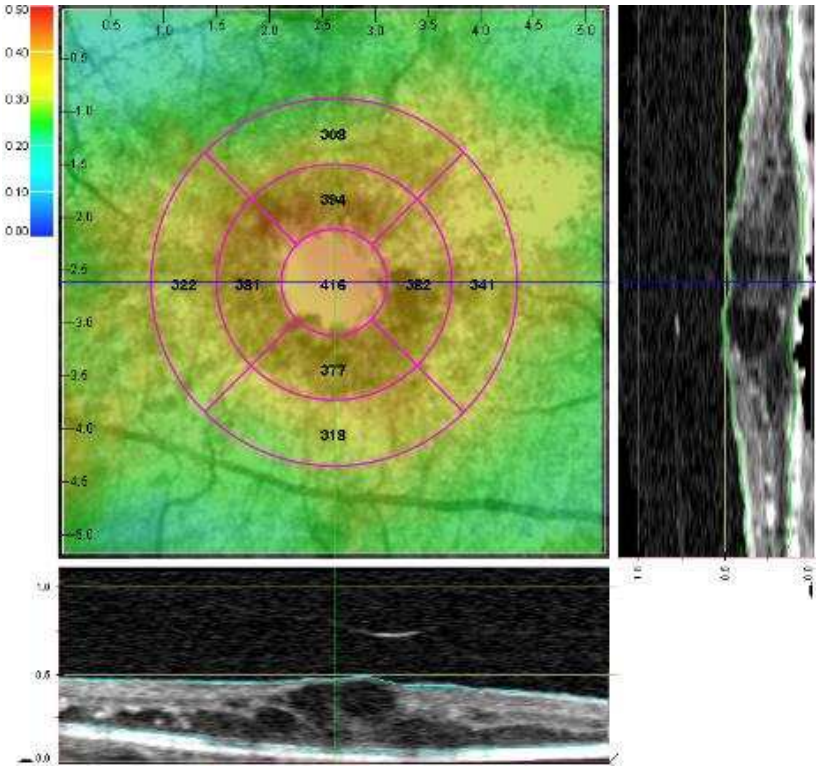


**Figure 3B**

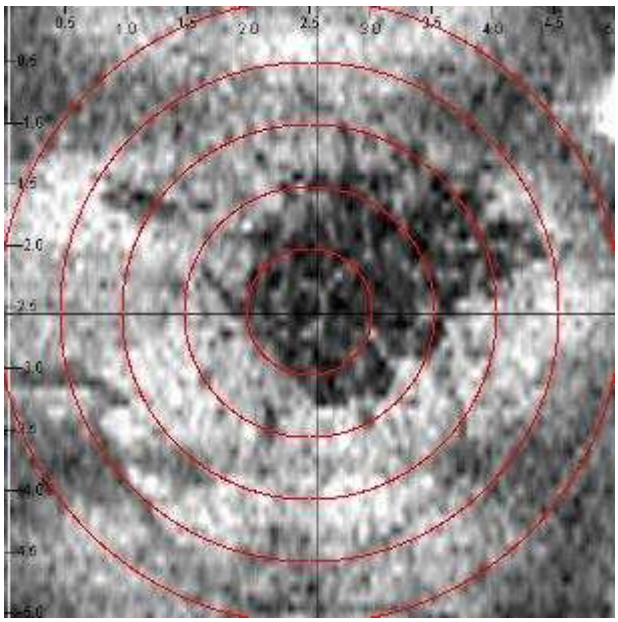

**Figure 4**

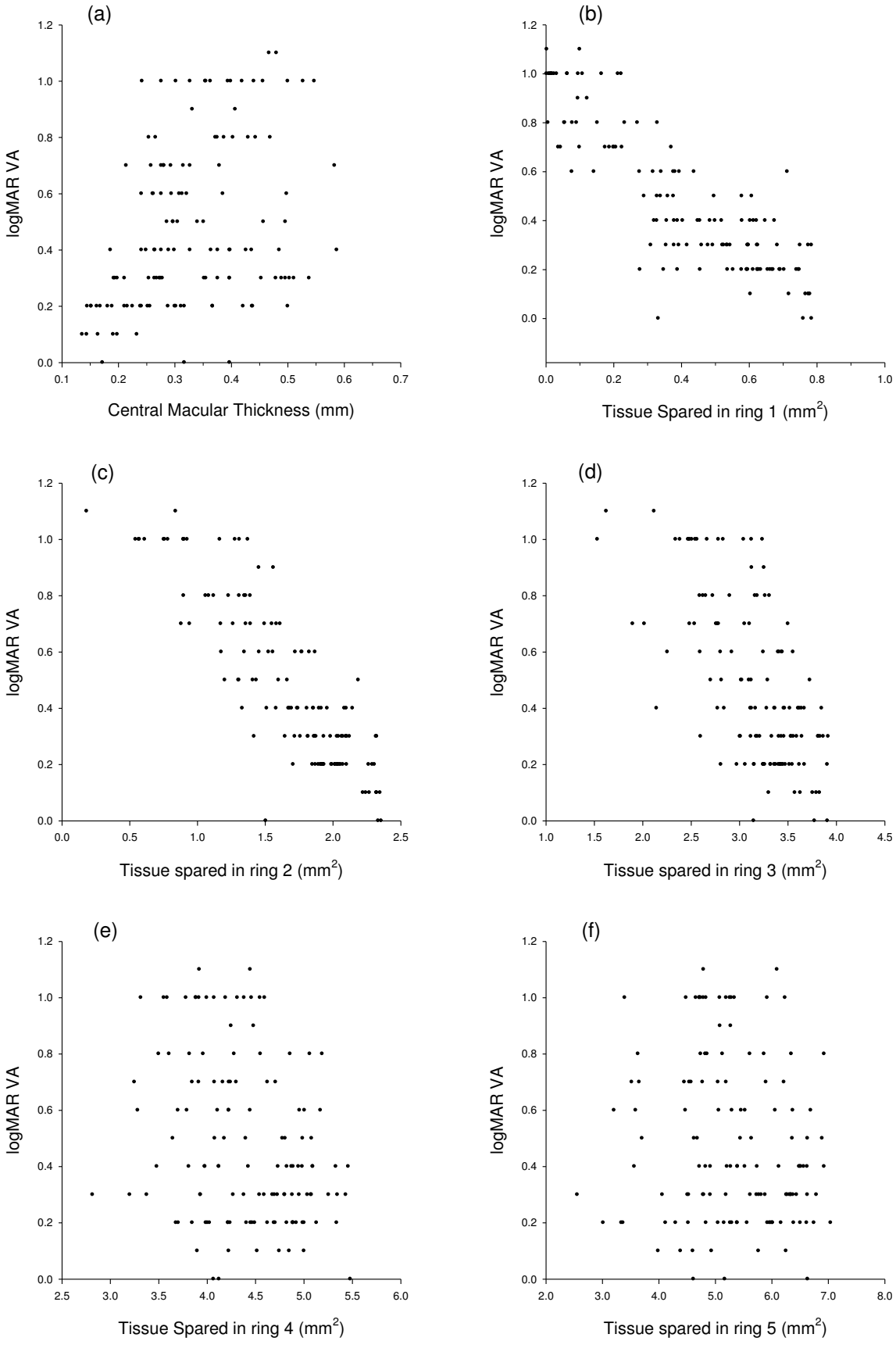
(a)
logMAR VA
Central Macular Thickness (mm)
(b)
logMAR VA
Tissue Spared in ring 1 (mm2)
(c)
logMAR VA
Tissue spared in ring 2 (mm2)
(d)
logMAR VA
Tissue spared in ring 3 (mm2)
(e)
logMAR VA
Tissue Spared in ring 4 (mm2)
(f)
logMAR VA
Tissue spared in ring 5 (mm2)

**Figure 5**

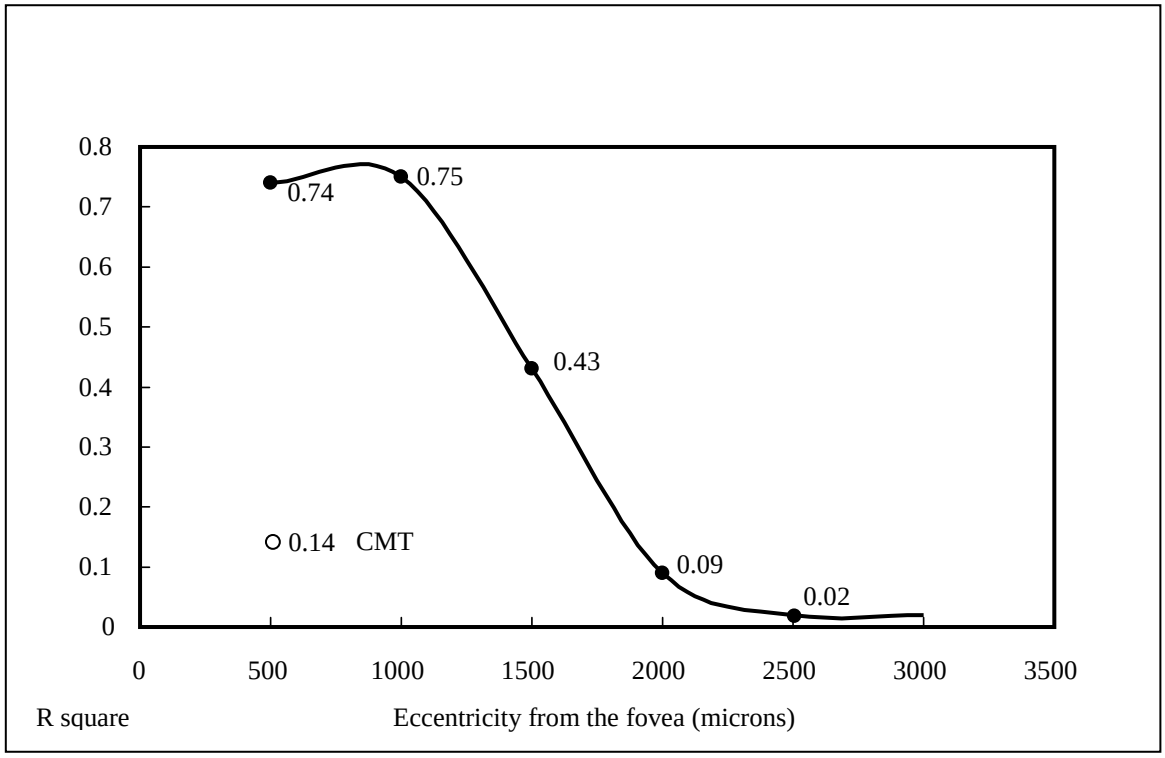
0.8
0.7
0.6
0.5
0.4
0.3
0.2
0.1
0
0.74
0.75
0.43
0.09
0.02
0.14 CMT
0
500
1000
1500
2000
2500
3000
3500
R square
Eccentricity from the fovea (microns)

**Figure 6**

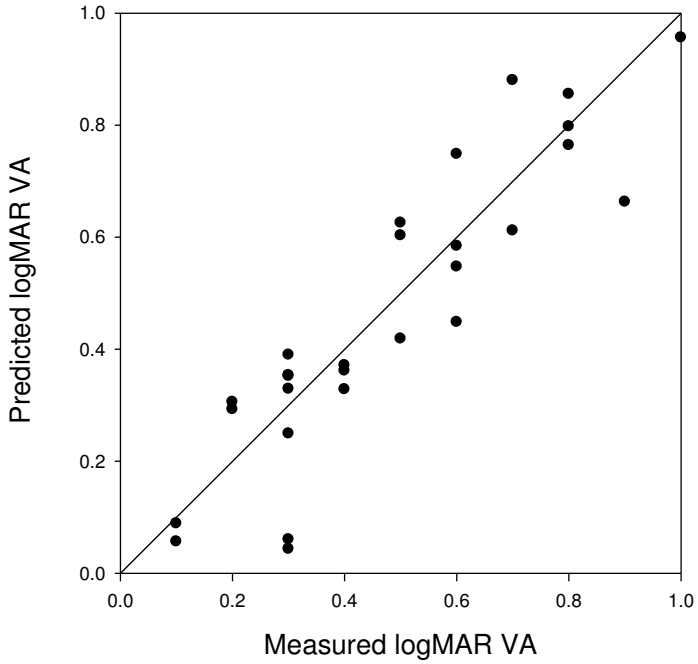


**Figure 7**

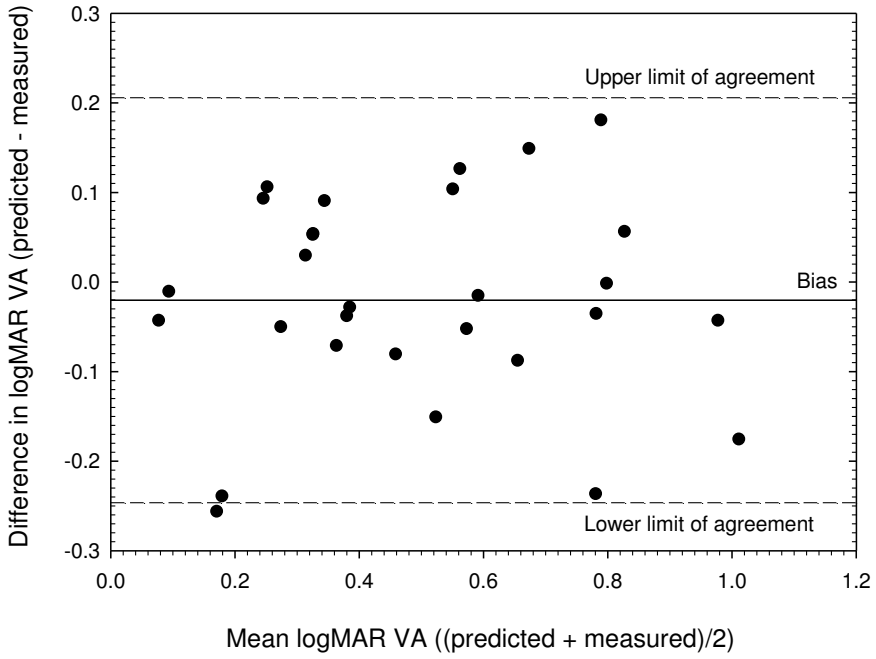

**Table 1**

| Patients 81 | Diagnosis | Unilateral 33 | Bilateral 48 |
|---|---|---|---|
| 60 | DMO | 14 cases | 46 cases |
| 12 | Uveitis | 10 cases | 2 cases |
| 6 | RVO | 6 cases | 0 cases |
| 2 | Irvine Gass | 2 cases | 0 cases |
| 1 | Tractional | 1 case | 0 cases |

**Table 2**

| Variable | rs | P (2-tailed) | $R^2$ (%) |
|---|---|---|---|
| CMT | +0.407 | <0.001 | 16.6% |
| Tissue spared in ring 1 (500µ) | -0.832 | <0.001 | 69.2% |
| Tissue spared in ring 2 (1000µ) | -0.841 | <0.001 | 70.7% |
| Tissue spared in ring 3 (1500µ) | -0.624 | <0.001 | 38.9% |
| Tissue spared in ring 4 (2000µ) | -0.277 | 0.001 | 7.7% |
| Tissue spared in ring 5 (2500µ) | -0.134 | 0.130 | 1.8% |